Something something something physics

Steven Green
of Emmanuel College

A dissertation submitted to the University of Cambridge
for the degree of Doctor of Philosophy

Abstract

LHCb is a b-physics detector experiment which will take data at the 14 TeV LHC accelerator at CERN from 2007 onward...

Declaration

This dissertation is the result of my own work, except where explicit reference is made to the work of others, and has not been submitted for another qualification to this or any other university. This dissertation does not exceed the word limit for the respective Degree Committee.

Andy Buckley

Acknowledgements

Of the many people who deserve thanks, some are particularly prominent, such as my supervisor…

Preface

This thesis describes my research on various aspects of the LHCb particle physics program, centred around the LHCb detector and LHC accelerator at CERN in Geneva.

For this example, I'll just mention Chapter **??** and Chapter **??**.

Contents

"Writing in English is the most ingenious torture ever devised for sins committed in previous lives."

— James Joyce

Chapter 1

Calorimeter Optimisation Studies

"There, sir! that is the perfection of vessels!"
— Jules Verne, 1828–1905

1.1 Calorimeter Optimisation Studies

If the future linear collider is to reach it's maximum potential in terms of energy resolution then, optimisation of the detector will be essential. The energy resolution in the particle flow paradigm is dependant upon several detector components. The momentum of charged particles arises from the shape of the tracks deposited within the detector while the energy of uncharged particles arise from calorimetric measurements. Application of sophisticated pattern recognition algorithms allows the particle type to be inferred for the charged particles. In tern this allows for the conversion of the track momentum into an energy measure for the charged particles. The particle identification algorithms use the topological information acquired from the calorimetric energy deposited to infer particle type for a subset of charged particles.

The calorimetric energy deposits are therefore used in a twofold manner: (i) as energy measurements for neutral particles and (ii) as input for particle identification algorithms. There is potential for significant gains to be made in physics performance by optimising the calorimeters due to their dominant role in energy measurements. In this chapter the optimisation of the calorimeters is considered. Parameters such

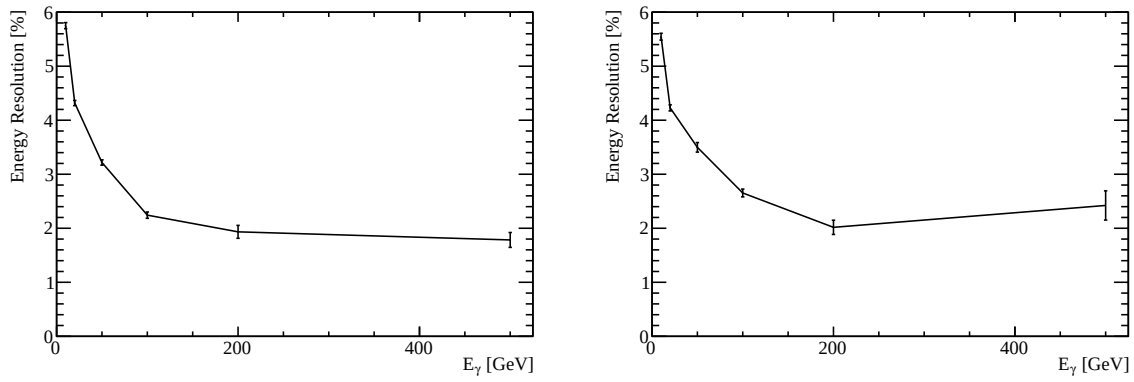

(a) Silicon active material, $5 \times 5\text{mm}^2$ ECal transverse granularity.

(b) Scintillator active material, $5 \times 5\text{mm}^2$ ECal transverse granularity.

Figure 1.1: Energy resolution as a function of photon energy for the nominal ILD detector for both the silicon and scintillator options.

as the longitudinal granularity, transverse granularity and material choices for the calorimeters are considered.

This chapter concludes with an optimisation of several global parameters for the detector. These parameters are not calorimeter specific, but the optimisation procedure developed for the calorimeters is appropriate to use. These parameters relate to the global detector size and the magnetic field applied throughout solenoid in the detector.

1.2 Metric

1.3 Simulation and Reconstruction

1.4 Calibration

1.5 Nominal Detector Performance

The energy resolution for single photon events as a function of photon energy, for the nominal ILD detector, is shown in figure 1.1. The nominal jet energy resolution can be found in section BLAH.

1.6 Electromagnetic Calorimeter Optimisation

The ECal primarily measures the energy deposits of electromagnetic showers. The default ILD detector model, summarised in table 1.1, contains 24 radiation lengths, which acts to confine all but the highest energy electromagnetic showers within it. The longitudinal structure of this default model is 29 readout layers, consisting of pairs of active and absorber material, and one presampling layer, which exists to encourage shower development. Increasing the thickness of the absorber material part way into the detector reduces the number of readout channels and cost of the overall calorimeter while retaining a high sampling rate at the start of particle showers, which is crucial for the pattern recognition aspect of particle flow calorimetry.

Parameter	Default Value
Transverse Granularity	$5 \times 5\text{mm}^2$ square cells
Longitudinal Granularity	29 Readout Layers, 1 Presampling Layers
Active Material Choice	Silicon or Scintillator
Active Material Thickness	0.5 mm (Silicon) or 2 mm (Scintillator)
Absorber Material Choice	Tungsten
Absorber Material Thickness	20 Layers of 2.1 mm followed by 9 Layers of 4.2 mm

Table 1.1: Cross section for selected processes for given value of α_4 and α_5 at 1.4 TeV.

The parameters being optimised in this study are:

- Transverse granularity or cell size. This is a vital aspect of the detector in the particle flow paradigm as smaller cell sizes give greater potential for being able to separate energy deposits from charged and neutral particles. This transverse granularity should have little to no effect on the intrinsic energy resolution of the detector.
- Longitudinal granularity or cell depth. This parameter dictates the intrinsic energy resolution of the detector as smaller cell depths mean more sampling is done of the particle shower and so, due to the Poissonian statistics governing the measurement of particle showers, the better the resolution.
- Active material choice. This is a choice between silicon or scintillator. As well as providing different intrinsic energy resolutions the readout mechanics of these

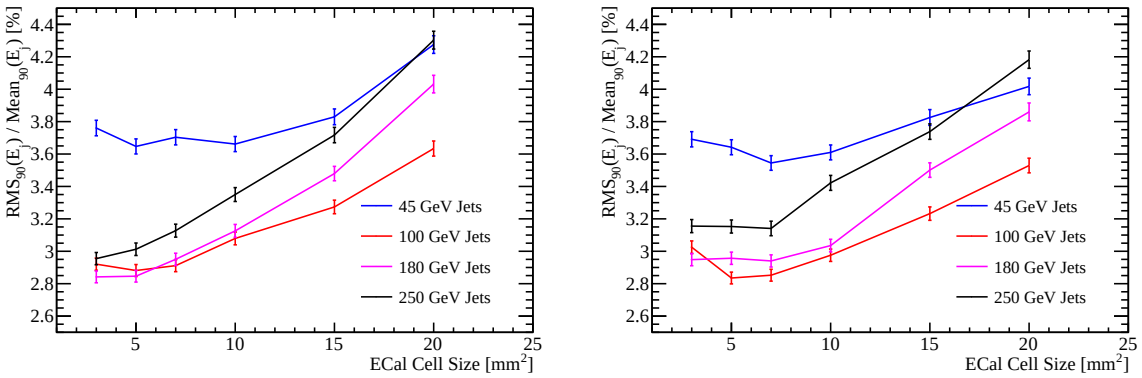

(a) Silicon active material. **(b)** Scintillator active material.

Figure 1.2: Jet energy resolution as a function of ECal cell size for the silicon and scintillator ECal options.

two options are significantly different. There is no clear prior knowledge as to which should provide better performance.

1.6.1 ECal Transverse Granularity

For this study a number of different detector models were considered where the transverse granularity in the ECal had been varied about the nominal value of $5 \times 5\text{mm}^2$ square cells. The granularities considered were $3 \times 3\text{mm}^2$, $5 \times 5\text{mm}^2$, $7 \times 7\text{mm}^2$, $10 \times 10\text{mm}^2$, $15 \times 15\text{mm}^2$ and $20 \times 20\text{mm}^2$ square cells for both the silicon and scintillator active material options. The jet energy resolution for these detector models as a function of transverse granularity in the ECal is shown in figure 1.3.

The jet energy resolution was found to improve with decreasing cell size. This is expected as smaller cell size lead to better separation of energy deposits from neutral and charged particle showers.

By examining the breakdown of the jet energy resolution into intrinsic resolution and confusion terms, as explained in chapter BLAH, it is possible to conclude that the dominant factor affecting the jet energy resolution when the transverse granularity of the ECal is varied is the confusion arising from photon energy deposits. Examples of jet energy resolution breakdowns are shown for 45 and 250 GeV jets for both the silicon and scintillator ECal options in figure 1.3. As expected in the intrinsic energy resolution does not change significantly with the transverse granularity.

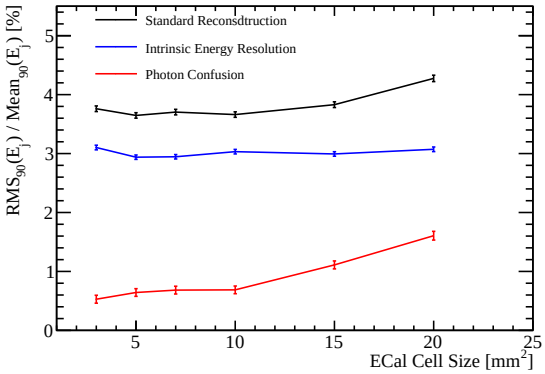

(a) Silicon active material, 45 GeV Jets.

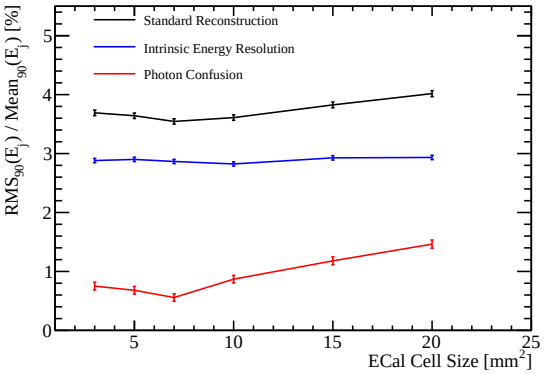

(b) Scintillator active material, 45 GeV Jets.

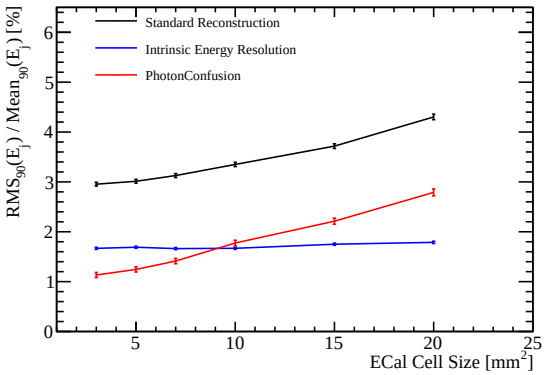

(c) Silicon active material, 250 GeV Jets.

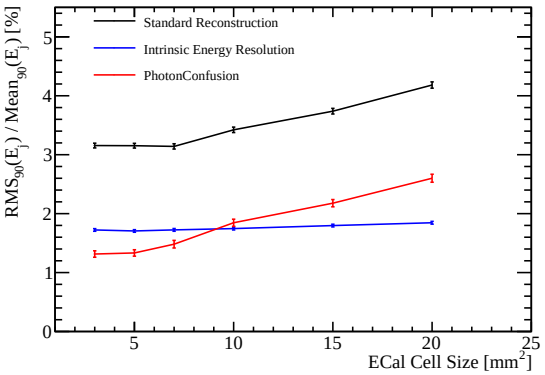

(d) Scintillator active material, 250 GeV Jets.

Figure 1.3: Jet energy resolution breakdown as a function of ECal transverse granularity for 45 and 250 GeV jets. Results are given for both the silicon and scintillator ECal options.

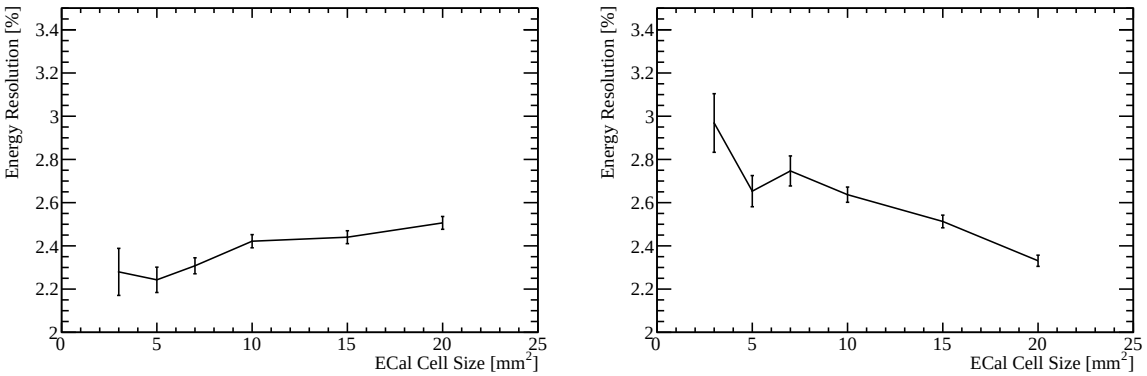

(a) Silicon active material, 100 GeV γ. **(b)** Scintillator active material, 100 GeV γ.

Figure 1.4: Energy resolution as a function of ECal transverse granularity for 100 GeV photons. Results are given for both the silicon and scintillator ECal options.

A more targeted test of the intrinsic energy resolution of the ECal is presented in figure 1.4, which examines the energy resolution of single photon samples at 100 GeV. For the silicon option the intrinsic energy resolution was found to not vary significantly across the transverse granularities under consideration, however, there is a degradation in energy resolution with increasing cell size for the scintillator option. This originates from an inactive region of material in the simulation that represents the multi pixel photon counter (MPPC). The MPPC occupies a fixed area of the cell irrespective of cell size and so fractionally the "dead" region of the cell increases as cell size is reduced (cite this somehow). These trends will be present in the jet energy resolution studies, however, as only a small fraction, $\approx 10\%$, of the jet energy arises from the ECal these trends will be washed out when looking purely at jets.

In conclusion smaller transverse granularities in the ECal significantly improve the jet energy resolution for both the silicon and scintillator options. The intrinsic energy resolution of the ECal is largely invariant to changes in the transverse granularity for the silicon option, while larger transverse granularities are beneficial to the scintillator option as they reduce the impact of "dead" regions of the detector.

1.6.2 ECal Longitudinal Granularity

For this study a number of different detector models were considered where the longitudinal granularity of the ECal absorber material, which in all cases is tungsten, had been varied about the nominal value for both the silicon and scintillator active

material options. In all cases the active layer thicknesses were left unchanged, that is 0.5 mm for the silicon option and 2 mm for the scintillator option. The layout of the ECal for detector models considered are summarised in table **??**.

Total Number of Layers	N_{Layers} Region 1	Absorber Depth Region 1	N_{Layers} Region 2	Absorber Depth Region 2	$N_{RadiationLengthsInAbsorber}$
29	20	2.10	9	4.20	22.77
25	17	2.40	8	4.80	22.60
19	13	3.15	6	6.30	22.47
15	10	4.00	5	8.00	22.31

Table 1.2: Transverse granularity layout of ECal models considered in this optimisation study. Radiation length of tungsten absorber is 3.504mm information from PDG.

Colophon

This thesis was made in LaTeX 2_ε using the "hepthesis" class [1].

Bibliography

[1] Andy Buckley. The hepthesis LaTeX class.

List of figures

List of tables